An Integrated Acousto-Mechanical Energy Approach for Monitoring Flexural Bond-Slip Behaviour of GFRP Bars and Concrete

AMER ILIYAS RATHER, SAUVIK BANERJEE
and ARGHADEEP LASKAR

ABSTRACT

Mechanical testing data and acoustic emission (AE) data can be independently analysed to evaluate the bond deterioration process of glass fibre reinforced polymer (GFRP) rebars and concrete. However, one type of data may not be adequate for thorough and accurate damage characterization and assessment. Sentry function, a unitless quantity, which relates mechanical and AE energy, has been efficiently applied in polymer composites and multi-layered laminates to study damage progression, including delamination. The sentry function has not been used in any of the past studies to understand the bond-slip behaviour of reinforcements in concrete. The present study attempts to exploit the effectiveness of the sentry function to evaluate the flexural bond-slip behaviour of GFRP rebar and concrete. A thorough AE monitoring experimental programme has been conducted to evaluate and understand the interfacial bond deterioration process between GFRP reinforcement and concrete under flexural loading. The experimental test variables include confinement conditions and embedment length of the GFRP bar. Findings from the study suggest that the sentry function proves to be a successful and effective tool for evaluating the GFRP-concrete flexural bond deterioration. The sentry function captures and delineates the development and utilization of various bond stress transfer mechanisms (chemical adhesion, mechanical interlocking, and frictional resistance) involved in bond-slip behaviour.

INTRODUCTION

Over the last decade, fibre-reinforced polymer (FRP) reinforced concrete (RC) structural parts have seen increased demand in critical civil infrastructure applications. The inherent advantages of FRP composites, such as exceptional mechanical properties

Amer Iliyas Rather, Department of Civil Engineering, Indian Institute of Technology Bombay, Powai, Mumbai, 400076, India
Sauvik Banerjee, Department of Civil Engineering, Indian Institute of Technology Bombay, Powai, Mumbai, 400076, India
Arghadeep Laskar, Department of Civil Engineering, Indian Institute of Technology Bombay, Powai, Mumbai, 400076, India

(stiffness-to-weight ratios), extraordinary corrosion resistance, and ease of production, handling, and installation procedures, make it a suitable substitute for conventional carbon steel in corrosive environments. However, because the use of FRP composites in structural applications is still relatively new, ACI 440.2R-08 recommends careful monitoring of these FRP-reinforced structures for at least ten years during service conditions. Bond degradation and deterioration of these components is one of the major concerns to be considered while developing design guidelines or standards and monitoring procedures for using FRP rebar in RC constructions. The bond-slip behaviour of steel RC is shown to differ from that of FRP RC. The surface geometric characteristics, configuration, and the mechanical properties of FRP rebar are considered to be the major causes of the divergence in the bond behaviour between concrete and steel rebar from the bond behaviour between concrete and FRP rebar. In addition to concrete strength, other factors such as confinement conditions, type of loading, and embedment length influence the bond strength of a FRP RC member. Chemical adhesion of the cementing material to the rebars, mechanical interlocking, and frictional resistance between the rebar and the concrete (including rib bearing on FRP bars) together contribute to the development of the interfacial bonding stress. Each of these aspects contributes differently to the total bond strength, initiating with chemical adhesion and progressing to the other two mechanisms that contribute to the pull-out strength of the bar during slippage. Various test methods have been devised to assess the bond strength of FRP RC members experimentally. Beam-based tests that closely simulate the practical structural loading/stress conditions are most suited to evaluate the bond strength of members.

Acoustic emission (AE) is a passive damage detection and monitoring technique in which the source signal is recorded for detection due to the progressive damage and degradation in a structural element [1]. Various researchers have recently used AE monitoring to assess bond integrity and quantify bond deterioration between concrete and rebars like steel [2], glass FRP [3], basalt FRP [4], and carbon FRP [5]. All these studies have only used AE-based parameters to quantify the bond deterioration process. One of the important AE signal parameters that is commonly used is AE energy. The AE energy (E_i) of a signal is frequently calculated as a straightforward time integral of the absolute signal voltage over time. Various studies by Saliba and Mezhoud [6] investigated the bond behaviour of steel and concrete under pull-out tests using AE energy and various other AE parameters. Studies conducted by [7], [8] have used AE energy to investigate corrosion-induced debonding phenomenon between steel/corroded steel and concrete under pull-out tests.

However, it has been observed that a thorough and accurate damage characterization and assessment of the structural element can be done if AE energy is analysed together with the mechanical/fracture energy developed during the loading or fracture process. Experimental investigations were conducted on concrete specimens to correlate AE energy and fracture energy in order to quantify the damage and deterioration in the test specimens [9]. The relationship between AE and mechanical/fracture energy has also been evaluated in recent studies using a function referred to as the sentry function (shown in Equation 1).

$$f(x) = ln\left[\frac{E_m(x)}{E_{AE}(x)}\right] \quad (1)$$

Where x is the displacement, mechanical energy is represented by the area under the load versus deflection curve and denoted by $E_m(x)$, and the cumulative value of AE energy is denoted by $E_{AE}(x)$. The sentry function has been mainly used to understand laminated composites' bond deterioration or delamination process [10]. Figure 1(a) depicts a typical representation of the sentry function, while Figure 1(b) illustrates its typical behavior during the bond deterioration process. The sentry function can exhibit one of four trends, depending on the extent of structural damage (as shown in Figure 1). The sentry function may exhibit one of four trends depending on the level of structural damage (see Figure 1). An upward inclination (PI) indicates that the structural element remains without any visible damage or microscopic damage in the material. A sharp drop (PII) suggests significant deterioration in the material. A constant trend (PIII) indicates a balance between degradation processes, such as damages, and strengthening mechanisms, such as fiber bridging. A steadily decreasing trend (PIV) signifies a gradual reduction in the load-carrying capacity of the composite structure. The term "BU" (Bottom-Up) refers to an instantaneous energy-storing capability induced by a strengthening event in the material. The first significant dip in the sentry function curve indicates the initiation of damage. Ichenihi et al. [11] employed the sentry function to investigate the damage mechanisms and progression affecting pseudo-ductility and mechanical response of thin-ply carbon/glass hybrid composites. Some studies have also used the sentry function to study the fracture evolution of FRP-strengthened RC members [12]. The sentry function was susceptible to their various damage states.

Since the delamination process closely relates to the rebar debonding in concrete, the sentry function could be used to investigate the debonding or bond-slip behaviour of rebars in RC elements. The present study attempts to exploit the capabilities of the sentry function to evaluate the flexural bond-slip behaviour of GFRP rebars and concrete. A thorough experimental program has been conducted to evaluate and understand the interfacial bond deterioration process between GFRP rebars and concrete under flexural loading through AE monitoring. Experimental test variables include confinement conditions and embedment length of the GFRP bar. Findings from the study suggest that the sentry function proves to be a successful and effective tool for evaluating GFRP-concrete bond deterioration. The sentry function captures and delineates the development and utilization of various bond stress transfer mechanisms (chemical adhesion, mechanical interlocking, and frictional resistance) involved in the bond-slip behaviour of GFRP RC members.

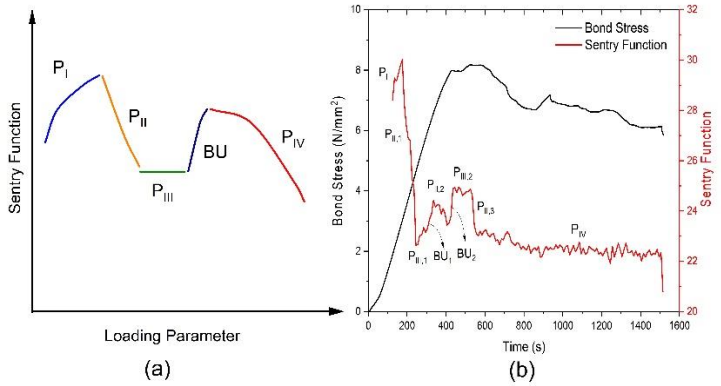

Figure 1. Typical representation of sentry function

EXPERIMENTAL PROGRAM

The materials, test specimens, and experimental procedures used in the present study to assess the bond behavior of GFRP-RC specimens under flexural loading are discussed in the sections below.

Specimen and Materials Specifications

The specimens tested in the present study have been designed as per guidelines for flexural bond testing of rebars and concrete provided by the RILEM committee. Figure 2 shows the dimensions and details of the tested specimens. A total of four test specimens have been tested in the present study. The embedment length of the GFRP bar has been kept equal to ten times the diameter of the bar (10d) in two of the tested specimens (named HS-10d-WC-S2 and HS-10d-NC-S2) and five times the diameter of the bar (5d) in the remaining two test specimens (named as HS-5d-WC-S2 and HS-5d-NC-S2). Out of the two specimens having 10d and 5d embedment lengths of GFRP rebars, one specimen has been designed with confinement reinforcement (WC), and the other has been designed without confinement reinforcement (NC).

GFRP rebars and concrete have been used for the fabrication of the test specimens in the present study. 12 mm diameter (nominal) GFRP rebar with tensile strength, Young's modulus, and percentage elongation equal to 955.67 MPa, 51.27 GPa, and 3.08%, respectively, have been used. ASTM D7205 [13] guidelines have been utilized to determine the mechanical properties of the GFRP rebar. M60 grade (high strength - HS) concrete has been used for casting the test specimens. The mix design for concrete has been performed as per IS 10262:2019 [14]. The confinement reinforcement has been provided in two specimens using 8 mm diameter longitudinal steel rebar and 6 mm diameter steel stirrups.

Experimental Procedure and Instrumentation.

The specimens have been tested under four-point loading conditions as per RILEM recommendations using a servo-controlled 500 kN actuator. A loading rate of 0.6 mm per minute and a sampling rate of 5 Hz have been adopted during the experimental program. Two load cells beneath the specimen supports, and a linear potentiometer (LP) attached to the GFRP bar has been used to measure the applied load and the bar slip (with respect to concrete), respectively (see Figure 2).

The AE instrumentation used during the testing of the specimens consisted of eight channel MISTRAS Micro-II Express 8 system with six R6D broadband differential AE sensors. Six sensors, three placed at the bottom and three placed on the side of the specimens, have been used (see Figure 2). A sampling rate of 2 MSPS was used during the tests. Trial tests have been carried out prior to the execution of the main experiments for noise calculations and instrument calibration. A fixed, pre-set threshold value of 48 dB has been used to filter out ambient and system noises. Other parameters to be defined in the AE system have been used as per recommendations and findings of previous literature.

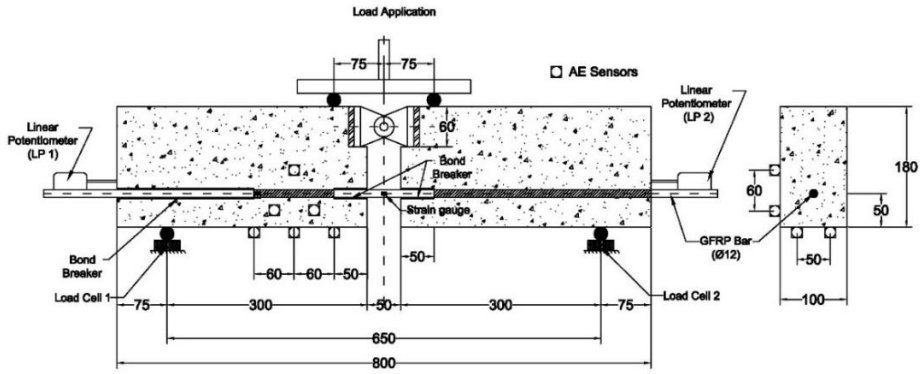

Figure 2. Dimensions (mm) and details of a typical specimen used during experimentation.

RESULTS AND DISCUSSION

AE Data Filtering

The raw AE data gathered during the testing of the specimens was filtered before the actual analyses of the data in order to remove noise-related, unwanted signals and irrelevant wave reflections occurring within the specimen edges. It has been observed that the actual AE signals with higher amplitudes are of longer durations and vice versa. So based on this hypothesis, the raw AE data obtained during the bond tests has then been processed and filtered using an amplitude-duration based filter, also known as the Swansong II filter. The filtering of the data was further enhanced by the use of an amplitude-rise time based filter. These filtering techniques (i.e., rejection limits) based on the amplitude-duration and amplitude-rise time used in the present study have been found very effective and have been previously used by other researchers [15], [16].

Acousto-Mechanical Response of the Specimens

Figure 3 shows the mechanical responses (bond-slip behavior) of the four tested specimens. The specimens have shown a typical bond-slip behavior with no or negligible initial slip at lower bond stress. A gradual increase has been observed in the slip of the GFRP bar as the bond stresses increase up to the peak bond stress. The increase in the slip values has been more rapid after the peak bond stress. The specimens with confinement (WC) have shown ductile behavior and have undergone pure pull-out failure without any splitting or failure of concrete. However, specimens without confinement (NC) have shown a brittle (abrupt) failure accompanied by the splitting of the concrete in the loaded area of the GFRP rebar. The failure pertaining to 5d specimens has been more rapid compared to that of the 10d specimens. In general, the bond strengths showed by the 5d and confined specimens have been more than that of the 10d unconfined specimens.

The AE response of the tested specimens has been shown in terms of the AE cumulative energy (AE-CE) in Figure 4. AE-CE has been observed to be negligible at the start of the tests, as the bond is perfectly intact. The minor events generated at this stage could be attributed to the hairline micro-cracking of the concrete. It has been subsequently observed that the AE energy starts to increase abruptly as the bond stress reaches the limiting stress value due to adhesion, thereby providing a clear indication of

the breaking of the chemical adhesion between the GFRP bar and the concrete. The AE-CE have increased as the bond deterioration increased and the specimens entered the peak stress region. The energy of the waves generated has increased substantially with a maximum value at the peak bond stress. The steps in the AE-CE curves can be clearly observed in Figure 4 as the tests have progressed. These have been related to the transitions between the various bond stress transfer mechanisms/stages (from chemical adhesion to mechanical interlocking and frictional resistance). A flat response in the AE-CE has been observed towards the end of the specimens test, indicating that the major contributing factors for bond stress transfer have been exhausted and the bond resistance to the external loads has significantly reduced. Similar observations was previously made for pull-out tests in SCC specimens conducted by Di et al. [3].

The Sentry function (discussed earlier) of the specimens that relate the mechanical energy and the acoustic energy of the specimens has also been plotted in Figure 4 with its variation with respect to bond stress and AE-CE of the specimens. An initial increase in the value of the sentry function has been observed corresponding to the PI definition of the function, which can be related to the chemical adhesion between the GFRP rebar and the concrete in the tested specimens. A subsequent drop in the sentry function has been observed corresponding to the PII definition of the function that can be related to the degradation of the chemical adhesion. Majorly ups with minor drops have been subsequently observed in the sentry function curves of the specimens up to the peak bond stress corresponding to the BUs and PIIs, respectively, of the sentry function and can be related to the development of new bond stress transfer mechanisms (mechanical interlocking of the ribs and concrete, and frictional resistance of rebar and concrete) and their corresponding depletion. A number of ups and downs have been observed since a large number of ribs of the rebar and aggregates of the concrete are involved in the development of the strengthening and degradation phenomenon. The sentry function has been majorly observed to deplete, indicating PIV part of the function. The depletion of the PIV part for the specimens with unconfined conditions, has been observed to be very abrupt and rapid indicating a brittle behavior. However, for the confined specimens, a more gradual process of PIV has been observed, with some parts of PIII (strengthening mechanisms balancing degradation phenomenon) also being present in the curves. It can be observed from the sentry function curves shown in Figure 4 that the energy-storing capabilities associated with 5d specimens is more rapid compared to that of 10d specimens (indicating a larger magnitude of BUs). This can be associated with comparatively less uniform stresses in 5d specimens to that of 10d specimens.

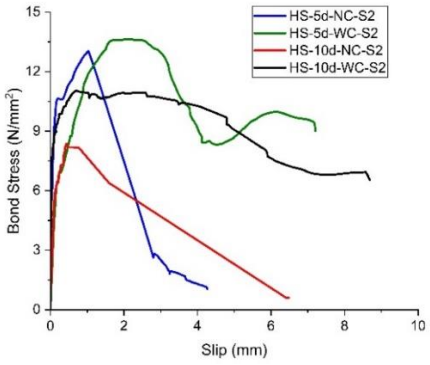

Figure 3. Bond-Slip behavior of the specimens.

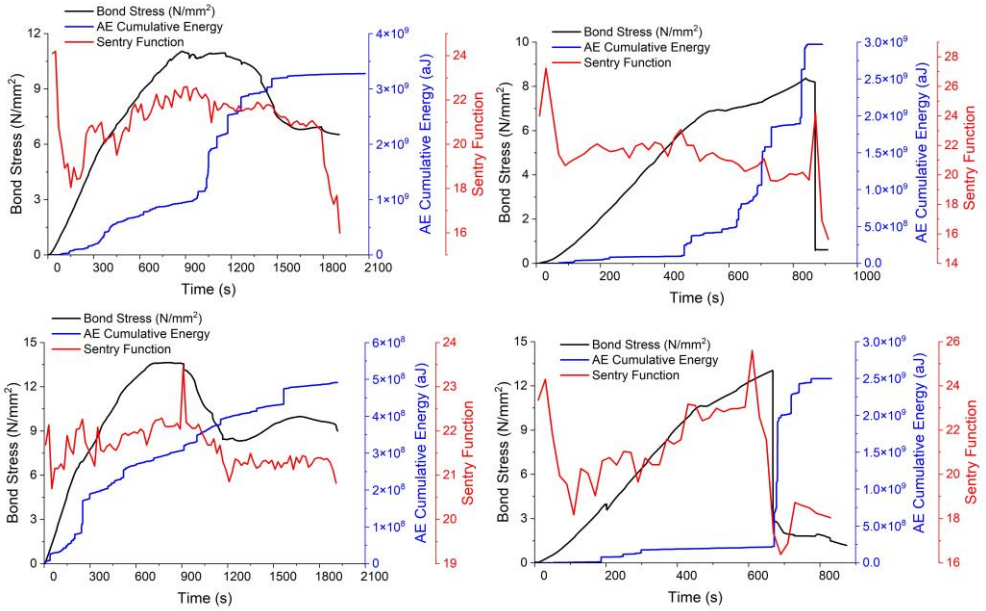

Figure 4. Variation of sentry function of the specimens with bond stress and cumulative AE energy of the specimens.

SUMMARY AND CONCLUSIONS

The present study offered a novel methodology to assess the flexural bond-slip behaviour of GFRP rebar and concrete by utilising the sentry function obtained from the AE signals generated during the four-point loading tests of GFRP RC specimens. A comprehensive experimental program integrating AE monitoring has been carried out in order to assess and comprehend the interfacial bond deteriorating process between GFRP rebars and concrete under flexural loads. The AE data analysis has been focussed on the acousto-mechanical energy-based sentry function in the present study. The major findings from the present study are given below.

- The bond-slip behaviour and AE-CE show a comparable variation with less energy at lower stress than rapid increases at peak stress. AE-CE shows the spikes as the stresses increase, indicating the bond stress transfer mechanism
- The Sentry function is able to capture various mechanisms associated with the GFRP concrete debonding phenomenon from the chemical adhesion to mechanical interlocking, and frictional resistance.
- The Sentry function can differentiate between the brittle and ductile mode of bond failure in the specimens associated with the confinement conditions of the specimens.
- The Sentry function changes also provide insights into the embedment length of specimens from 5d to 10d.

From the current study it can be concluded that the sentry function method is a useful tool for monitoring the bond deterioration phenomenon in GFRP RC members. However, it should be noted this being the first study to be conducted of this nature, more studies and more variations of parameters related to bond slip behaviour should be conducted for a better understanding and application of the sentry function in the monitoring of the bond deterioration process.

REFERENCES

1. Rather, A. I., P. Mirgal, S. Banerjee, and A. Laskar. 2023. "Application of Acoustic Emission as Damage Assessment Technique for Performance Evaluation of Concrete Structures : A Review," *Practice Periodical on Structural Design and Construction*, *28*(3). https://doi.org/10.1061/PPSCFX.SCENG-1256
2. Gallego, A., A. Benavent-Climent, and E.Suarez. 2016. "Concrete-Galvanized Steel Pull-Out Bond Assessed by Acoustic Emission," *Journal of Materials in Civil Engineering*, *28*(2):04015109. https://doi.org/10.1061/(asce)mt.1943-5533.0001372
3. Di, B., J. Wang, H. Li, J. Zheng, Y. Zheng, and G. Song. 2019. "Investigation of bonding behavior of FRP and steel bars in self-compacting concrete structures using acoustic emission method". *Sensors (Switzerland)*, *19*(1):1–14. https://doi.org/10.3390/s19010159
4. Chen, Y., and S. Chen. 2020. "Acoustic Emission Characteristics of Bond-Slip for BFRP Concrete at Different Loading Rates," *Russian Journal of Nondestructive Testing*, *56*(12):1030–1041. https://doi.org/10.1134/S1061830921010046
5. Yang, Y., Z. Li, T. Zhang, J. Wei, and Q. Yu. 2017. "Bond-Slip Behavior of Basalt Fiber Reinforced Polymer Bar in Concrete Subjected to Simulated Marine Environment: Effects of BFRP Bar Size, Corrosion Age, and Concrete Strength," *International Journal of Polymer Science*, 16–24. https://doi.org/10.1155/2017/5156189
6. Saliba, J. and D. Mezhoud, 2019. "Monitoring of steel-concrete bond with the acoustic emission technique," *Theoretical and Applied Fracture Mechanics*, *100*(February):416–425. https://doi.org/10.1016/j.tafmec.2019.01.034
7. Van Steen, C., E. Verstrynge, M. Wevers, and L. Vandewalle. 2019. "Assessing the bond behaviour of corroded smooth and ribbed rebars with acoustic emission monitoring," *Cement and Concrete Research*, *120*(March):176–186. https://doi.org/10.1016/j.cemconres.2019.03.023
8. Wang, L., J. Yi, H. Xia, and L. Fan. 2016. "Experimental study of a pull-out test of corroded steel and concrete using the acoustic emission monitoring method". *Construction and Building Materials*, *122*:63–170. https://doi.org/10.1016/j.conbuildmat.2016.06.046
9. Mirgal, P., R. K. Singh, and S. Banerjee. 2022. "Acoustic and Fracture Energy Correlation in Mode I Fracture with Concrete Damage Plasticity Model and Three-Point Bend Experiment,"*Journal of Material in Civil Engineering*. https://doi.org/10.1061/(ASCE)MT.1943-5533.0004673
10. Bakhtiary Davijani, A. A., M. Hajikhani, and M. Ahmadi. 2011. "Acoustic Emission based on sentry function to monitor the initiation of delamination in composite materials," *Materials and Design*, *32*(5):3059–3065. https://doi.org/10.1016/j.matdes.2011.01.010
11. Ichenihi, A., W. Li, and Y. Gao. 2021. "Damage analysis of combined continuous and discontinuous thin-ply carbon/glass hybrid composite using acoustic emission," *Polymer Composites*, *42*(12):6764–6776. https://doi.org/10.1002/pc.26337
12. Selman, E., A. Ghiami, and N. Alver. 2015. "Study of fracture evolution in FRP-strengthened reinforced concrete beam under cyclic load by acoustic emission technique: An integrated mechanical-acoustic energy approach," *Construction and Building Materials*, *95*:832–841. https://doi.org/10.1016/j.conbuildmat.2015.07.162
13. ASTM D7205/D7205. 2006. "Standard Test Method for Tensile Properties of Fiber Reinforced Polymer Matrix Composite Bars," *American Standard of Testing Materials*. https://doi.org/10.1520/D7205_D7205M-06R11
14. IS 10262. 2019. "Concrete Mix Proportioning — Guidelines," *Bureau of Indian Standards, New Delhi, India*.
15. Abdelrahman, M. A., M. K. ElBatanouny, J. R. Rose, and P.H. Ziehl. 2019. "Signal processing techniques for filtering acoustic emission data in prestressed concrete," *Research in Nondestructive Evaluation*, *30*(3):127–148. https://doi.org/10.1080/09349847.2018.1426800
16. ElBatanouny, M. K., A. Larosche, P. Mazzoleni, P. H. Ziehl, F. Matta, and E. Zappa. 2014. "Identification of Cracking Mechanisms in Scaled FRP Reinforced Concrete Beams using Acoustic Emission," *Experimental Mechanics*, *54*(1):69–82. https://doi.org/10.1007/s11340-012-9692-3